Korean J. Chem. Eng., **28**(2), 519-526 (2011)
DOI: 10.1007/s11814-010-0384-3

Examining the effects of velocity ratio of the pressurized flow to the main inlet flow on coagulants dispersion in pump diffusion mixer

No-Suk Park†, Seong-Su Kim, Kwan-Yeop Kim, and Sangyoung Park

Water Research Center, K-water Institute, Korea Water Resources Corporation (K-water),
462-1, Jeonmin-dong, Yusung-gu, Daejeon 305-730, Korea
(*Received 1 December 2009 • accepted 20 July 2010*)

Abstract−This study was conducted to evaluate the ratio of the pressurized flow to the main inlet flow, which has been considered one of the most important parameters for operating the pump diffusion mixer (PDM). Computational fluid dynamics (CFD) simulation was employed to evaluate the conventional operation rule of PDM and to propose a supplementary operating parameter and criterion. Test simulation of CFD was carried out for the 21 cases of flow ratio in a full scale PDM. The values of local velocity gradient were calculated in each case to analyze the simulation results in more detail. A wet test was conducted to verify CFD simulation results, which measures the factual coagulant dispersion distribution at a distance of 5.4 m from deflector. From results of both CFD simulation and wet test, the flow ratio was adequate as an operating parameter or criterion; also, the velocity ratio (dimensionless) of the pressurized flow to the main inlet was useful in predicting the performance of PDM. In addition, the injected coagulant could be dispersed evenly in overall cross section on the condition that the velocity ratio is at least over 20.

Key words: Pump Diffusion Mixer, Flow Ratio, Velocity Ratio, Computational Fluid Dynamics, Wet Test

INTRODUCTION

Rapid mixing is required in the water treatment process to rapidly disperse coagulant into raw water prior to flocculation, sedimentation and filtration process, which has a strong influence on the overall treatment efficiency. Since the hydrolysis products, $Me_l(OH)_m^{n+}$ (Me: Metal ions, OH: Hydroxide ion, *l*, m, n: constants) of the coagulants such as alum or Fe(III) are produced within a very short time of 10^{-4} to 1 second and since aluminum hydroxide starts to precipitate in about 7 seconds [1], it is important to make the metallic coagulants rapidly disperse into the whole fluid bulk. However, it is practically impossible to disperse them within a second and thus it is usually recommended that for efficient operation and design the coagulant be dispersed as rapidly as possible [2,3]. In addition, since mechanical mixing devices cannot disperse coagulants within such a short time, most operators increase the amount of coagulant determined in the laboratory by about 30-40% to get the required efficiency by increasing collision opportunities between coagulant ions and colloidal particles [4].

In many conventional treatment plants, however, coagulant mixing is typically performed in a concrete basin with a mechanical mixer; a retention time of 1-2 min is provided. Mechanical mixing with a longer retention cannot guarantee an instantaneous and even coagulant dispersion [5]. For this reason, the so-called pump diffusion mixer (PDM) has been proposed. PDM is a reasonable method and also has the potential to solve the problems of a conventional mechanical mixer, such as noise, energy waste and high maintenance cost. The previous work conducted using various rapid mixing devices to test the sedimentation performance showed that an in-line hydraulic jet and static mixers were able to achieve performance equivalent to that of the mechanical mixing type at lower coagulant dosages [6].

There have been a number of studies on a comparison of different rapid mixing devices and conditions. In contrast there have been relatively few studies on PDM optimization and the establishment of operating guidelines [4-6]. Most manufacturers have suggested that the ratio of the pressurized flow to the main inlet flow is the most important parameter in PDM operation. Also, Kawamura recommended that the flow ratio should be in the range of 4-10% in order to guarantee uniform coagulant dispersion in PDM [4]. Since the beginning of 2000 several water treatment plants in Korea have introduced PDMs as initial mixing step and operated them according to the manufacturer's suggestion. However, uneven dispersion of the injected coagulant is often observed in a full-scale PDM operated on the suggested conditions.

Therefore, the main purpose of this paper was to evaluate the effect of the ratio of the pressurized flow to the main inlet flow, which have been used one of the most important parameters for operating PDM, and to suggest a supplementary operating parameter and criterion for optimal operation.

MATERIAL AND METHODS

1. Methodology of CFD Simulation

In this study, computational fluid dynamics (CFD) simulation was carried out for 21 cases (refer to Table 1) of flow ratio in order to visualize the performance of a full-scale PDM, which is operating in Songjeon water treatment plant in Korea. The data acquiring line (red dot line in Fig. 1) was selected for derivation of the local velocity gradient, which can be extended to explain the results of wet test. Velocity and energy dissipation in each case were simulated

†To whom correspondence should be addressed.
E-mail: nspark@kwater.or.kr

Table 1. CFD simulation conditions

Case	Main inlet water flow rate (Qi) ($m^3\ h^{-1}$)	Main inlet water velocity (V1) ($m\ s^{-1}$)	Pressurized water flow rate (q2) ($m^3\ h^{-1}$)	Pressurized water velocity (V2) ($m\ s^{-1}$)	Flow ratio (%)	Velocity ratio (dimension less)
Case 1	725	0.1781	73.1	4.311	10	24.2
Case 2	1,450	0.3562	92.2	5.437	6.4	15.3
Case 3	2,175	0.5345	105.5	6.222	4.9	11.6
Case 4	2,900	0.7126	116.1	6.847	4.0	9.6
Case 5	4,350	1.0689	132.9	7.838	3.0	7.3
Case 6	1,041	0.2558	31.23	1.842	3.0	7.2
Case 7	1,041	0.2558	62.46	3.684	6.0	14.4
Case 8	1,041	0.2558	93.69	5.525	9.0	21.6
Case 9	1,041	0.2558	124.92	7.367	12.0	28.8
Case 10	2,028	0.5116	60.84	3.588	3.0	7.2
Case 11	2,028	0.5116	121.68	7.716	6.0	14.4
Case 12	2,028	0.5116	182.52	10.764	9.0	21.6
Case 13	2,028	0.5116	243.36	14.352	12.0	28.8
Case 14	3,123	0.7674	93.69	5.526	3.0	7.2
Case 15	3,123	0.7674	187.38	11.051	6.0	14.4
Case 16	3,123	0.7674	281.07	16.577	9.0	21.6
Case 17	3,123	0.7674	374.76	22.102	12.0	28.8
Case 18	4,164	1.0232	124.92	0.737	3.0	7.2
Case 19	4,164	1.0232	249.84	1.473	6.0	14.4
Case 20	4,164	1.0232	374.76	22.101	9.0	21.6
Case 21	4,164	1.0232	499.68	29.468	12.0	28.8

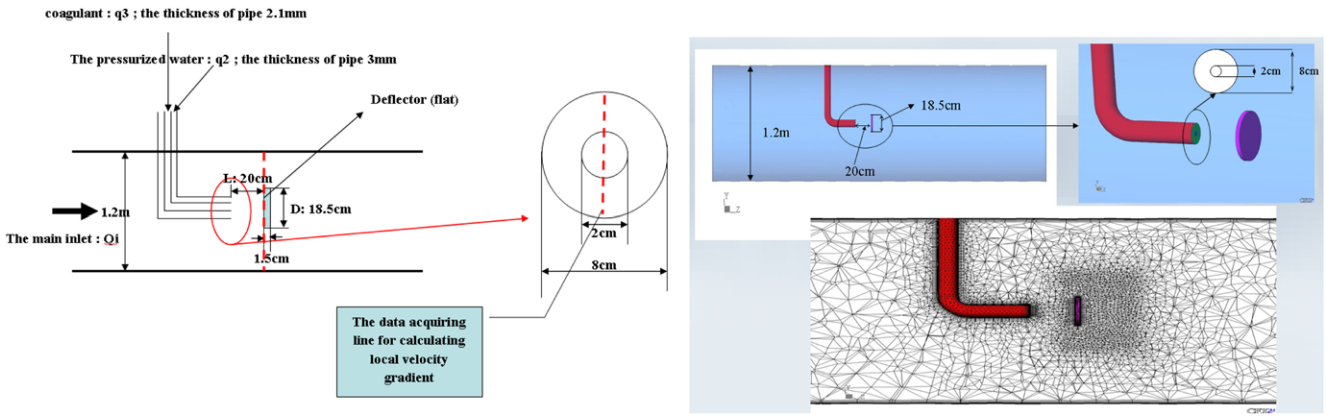

Fig. 1. The structural features of the selected full scale PDM and mesh for CFD simulation.

using commercial CFD code, CFX 10.0 developed by ANSYS [7]. Fig. 1 shows the structural features of the selected full-scale PDM and mesh for CFD simulation. The CFD simulation works by splitting the geometry of interest into a large number of elements, collectively known as 'grids' or 'cell'. Then, momentum and continuity equations were formulated for each grid together with given boundary conditions, and then repeatedly solved by using FVM (finite volume method) [8].

In this simulation, 200,000 cells in tetra shape were generated for the geometry of the PDM as shown in Fig. 1. The time-averaged Navier-Stokes equations for momentum and continuity were solved in this study for steady, incompressible, turbulent and isothermal flow.

The continuity and momentum equations are, respectively, as follows:

$$\nabla\cdot(\underline{U})=0 \quad \text{(i)}$$

$$\nabla\cdot(\rho\underline{U}\otimes\underline{U}-\mu\nabla\underline{U})=\underline{B}+\nabla P-\nabla\cdot(\overline{\rho\underline{u}\otimes\underline{u}}) \quad \text{(ii)}$$

Where ρ and μ are the fluid density and dynamic viscosity, respectively; P the pressure; $\underline{U}$ the fluid mean velocity; $\underline{B}$ a body force; and $\underline{u}$ the fluctuating velocity.

All cases were simulated by using turbulence modeling in order to investigate eddy flow and energy dissipation in more detail. Therefore, the RNG k-ε model was used for modeling the turbulence transport of momentum. Also, on the pipe wall surface, no-slip condition was assumed, and the well-known standard wall boundary method was applied to bridge the viscous sub-layer [9].

Table 1 summarizes 21 cases of flow ratio to simulate the hydrodynamic behavior in the selected full-scale PDM. Cases 1-5 were determined based on the manufacturer's suggestion. On the other hand, cases 6-21, in which flow ratio was altered 3-12% on the fixed inlet velocity, were selected in order to investigate the effect of flow ratio on the performance of PDM in detail.

2. Wet Test

Wet tests were conducted to investigate the factual coagulant dispersion phenomena within PDMs on the different velocity ratio. The zeta-potential was measured all over the cross section at a distance of 4.5D (D=1,200 mm) from the deflector in the selected PDMs for various conditions of the ratio of the pressurized flow to the main inlet flow (refer Fig. 2). The distance of 4.5D was determined due to the results of CFD simulation. The results showed in advance that a distance of 4.5D is enough to develop the main flow fully and stabilize it from the deflector. The coagulant being used in the selected Songjeon WTP is PAHCS (10.5%). Samples were taken from total 29 points all over the cross section (refer Fig. 2). The zeta potential of each sample was measured with a zeta meter (Malvern Ltd., Model Zen 2600, U.K). The wet test was carried out for three conditions on which flow ratio and velocity ratio were 2% (dimensionless: 5.6), 4% (dimensionless: 11.1) and 8% (dimensionless: 22.2), respectively. Zeta potential results in each case were made graphs using commercial program, SURFER 8.0. These graphs show the actual coagulant dispersion distribution on the selected overall section.

RESULTS AND DISCUSSION

1. Results of Wet Test

1-1. Case of Velocity Ratio 5.6 (Dimensionless)

Wet tests were conducted in order to investigate the factual coagulants dispersion phenomena on three different conditions. Fig. 3 shows the factual zeta potential distribution at a distance of 5.4 m from deflector in the case that the velocity ratio was 5.6 for different main inlet water flow rates, 3,250 $m^3 h^{-1}$ and 1,625 $m^3 h^{-1}$, respectively. Compared with each other, the case (b) in Fig. 3 shows a higher zeta-potential distribution in the central region than the case (a). However, even though there is a little difference between two distribution patterns, it is common that the measured zeta potential was higher on the lower part than that of the upper part in both cases. Especially, the zeta potential was below −10 mV on the upper-right part. On the other hand, the zeta potential was negative on the upper part, which resulted from the concentration of coagulant being rare

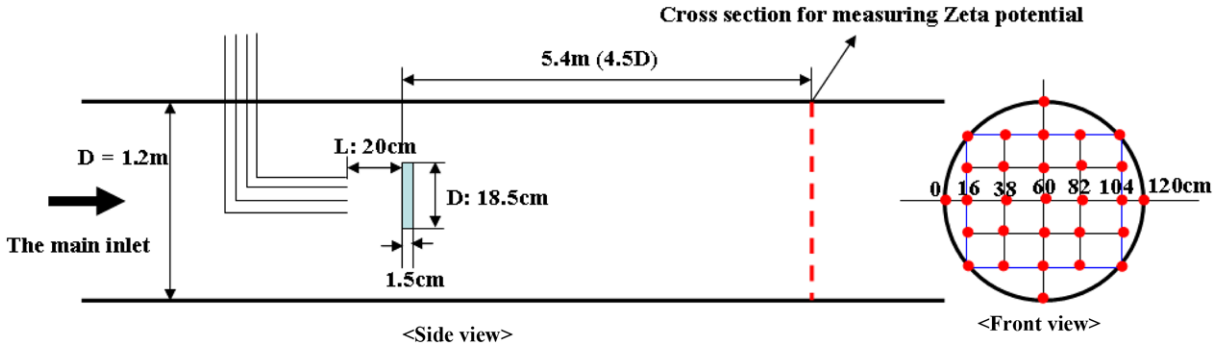

Fig. 2. The schematic of wet test.

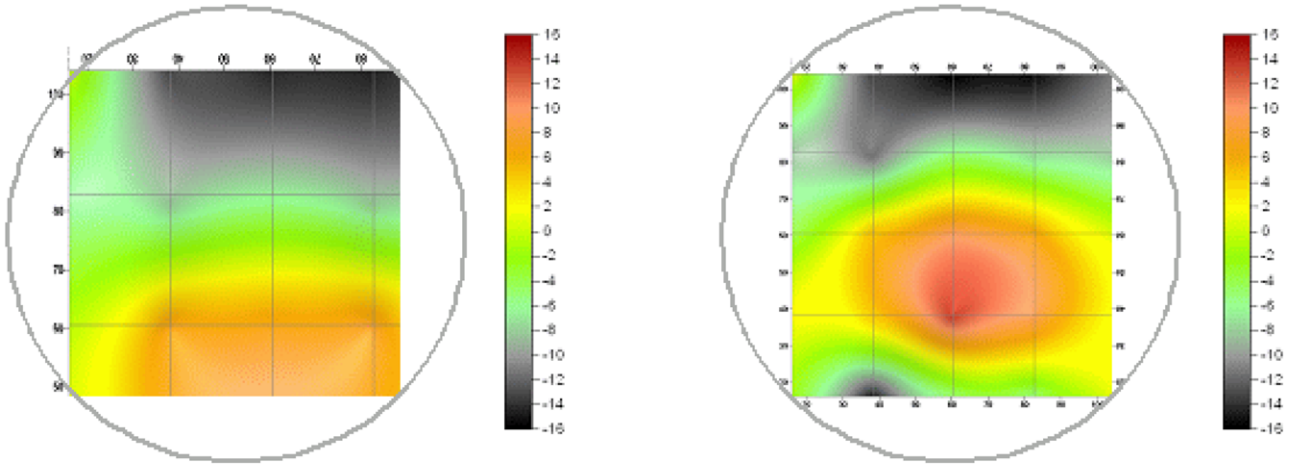

Fig. 3. Zeta potential distribution pattern in the case of velocity ratio 5.6. (a) The main inlet water flow rate: 3,250 $m^3 h^{-1}$, The pressurized water flow rate: 65 $m^3 h^{-1}$ (velocity ratio: 5.6). (b) The main inlet water flow rate: 1,625 $m^3 h^{-1}$, The pressurized water flow rate: 32.5 $m^3 h^{-1}$ (velocity ratio: 5.6).

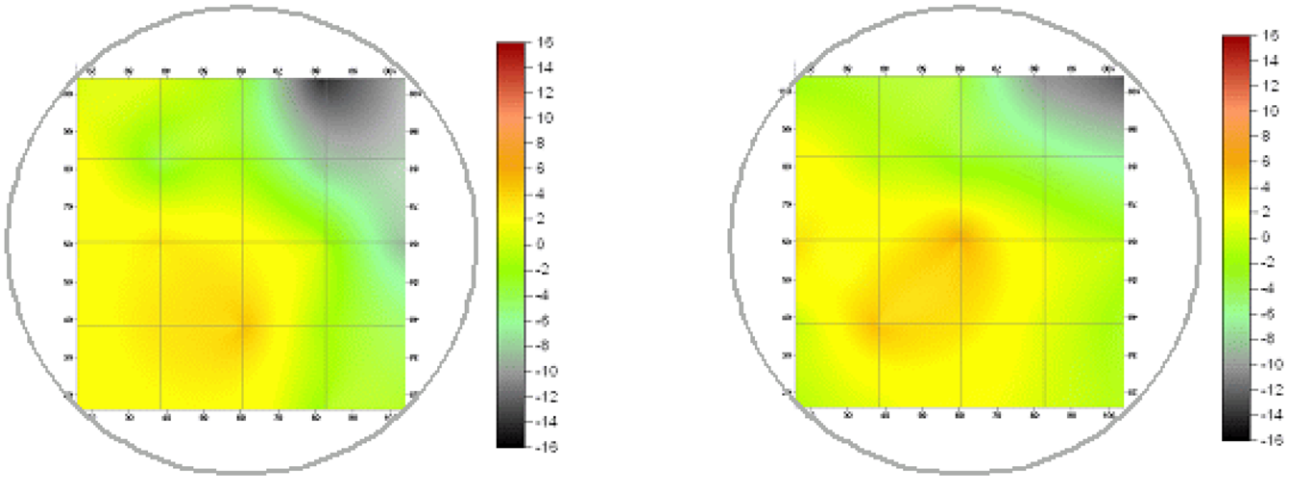

(a) (b)

Fig. 4. Zeta potential distribution pattern in the case of velocity ratio 11.1. (a) The main inlet water flow rate: 3,250 m^3/hr, The pressurized water flow rate: 130 m^3/hr (velocity ratio: 11.1). (b) The main inlet water flow rate: 1,625 m^3/hr, The pressurized water flow rate: 65 m^3/hr (velocity ratio: 11.1).

on the upper part. The reason why the zeta potential was higher on the lower part than upper part is that the injected coagulant was concentrated on the lower part.

1-2. Case of Velocity Ratio 11.1 (Dimensionless)

Fig. 4 shows the factual zeta potential distribution in the case that the velocity ratio was 11.1 for different main inlet flow rates, 3,250 $m^3\ h^{-1}$ and 1,625 $m^3\ h^{-1}$, respectively. Compared with the results from the case of velocity ratio 5.6, even though the distribution of zeta potential is relatively uniform, a negative zeta potential region existed on the upper right side of the measured cross section.

1-3. Case of Velocity Ratio 22.2 (Dimensionless)

Fig. 5 shows the factual zeta potential distribution in the case that the velocity ratio was 22.2 for the constant main inlet flow rate, 1,625 $m^3\ h^{-1}$. Compared with the results from the previous cases, the distribution of zeta potential is more uniform than any other case. Also, there is no negative zeta potential region all over the selected cross section.

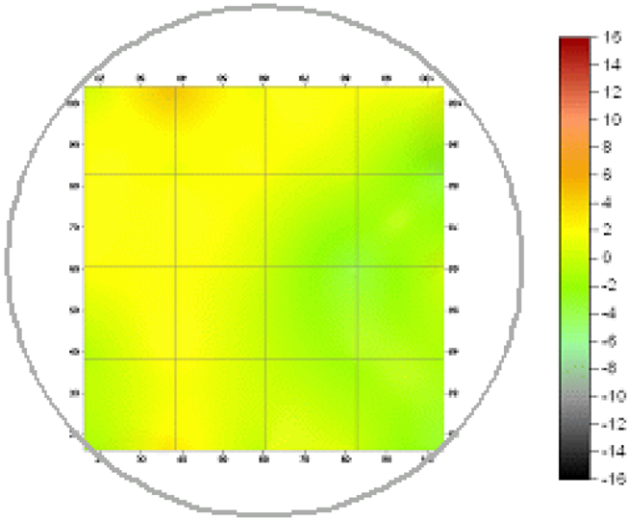

Fig. 5. Zeta potential distribution pattern in the case of velocity ratio 22.2 (The main inlet flow rate: 1,625 $m^3\ h^{-1}$, The pressurized flow rate: 130 $m^3\ h^{-1}$ (velocity ratio: 22.2).

The results of the wet test are versatile to verify the CFD simulation results, which are discussed in the next section, "Results of CFD simulation," and they are in good accordance with each other. From both results, it can be concluded that the flow ratio was adequate as operating parameter or criterion; also the velocity ratio of the pressurized flow to the main inlet flow (dimensionless) was useful in predicting the performance of PDM. Also, if the velocity ratio is at least over 20, the performance of PDM, ultimately the uniform dispersion of coagulant, can be guaranteed.

2. Results of CFD Simulation

Fig. 6 shows the results of CFD simulation for the cases 1-5 based on various flow ratio according to the manufacturer's suggestion.

As shown in Fig. 6, while flow ratio decreases from case 1 to case 5, and the pressurized water velocity increases from 4.311 m s^{-1} to 7.838 m s^{-1}, turbulent flow seems to increase gradually in the overall main pipe including the rear region of deflector. On the condition of the same geometry and identical fluid properties, the extent of turbulence is totally depending on the magnitude of velocity. In Fig. 6, the pressurized water velocity increases from case 1 to 5, the magnitude of velocity increase gradually in the overall pipe. To analyze the results of CFD simulation in more detail, local velocity gradient values were calculated on the data acquiring line close to the deflector (refer Fig. 1). The local velocity gradient concept in unit process was suggested as shown in Fig. 7 [10].

Fig. 8 shows the profiles of the calculated velocity gradient on the data acquiring line in cases 1-5.

Fig. 9 shows the relationship between the flow rate ratio and the average of local velocity gradients. As shown in Fig. 9, the less the flow ratio becomes, the larger the local velocity gradient becomes. This might be because even though flow ratio decreases, the actual pressurized water velocity increases as mentioned above.

To investigate these phenomena in more detail, the cases from 6 to 21 described in Table 1 were simulated. Fig. 10 shows the simulation results of cases 6 and 21 as the representatives.

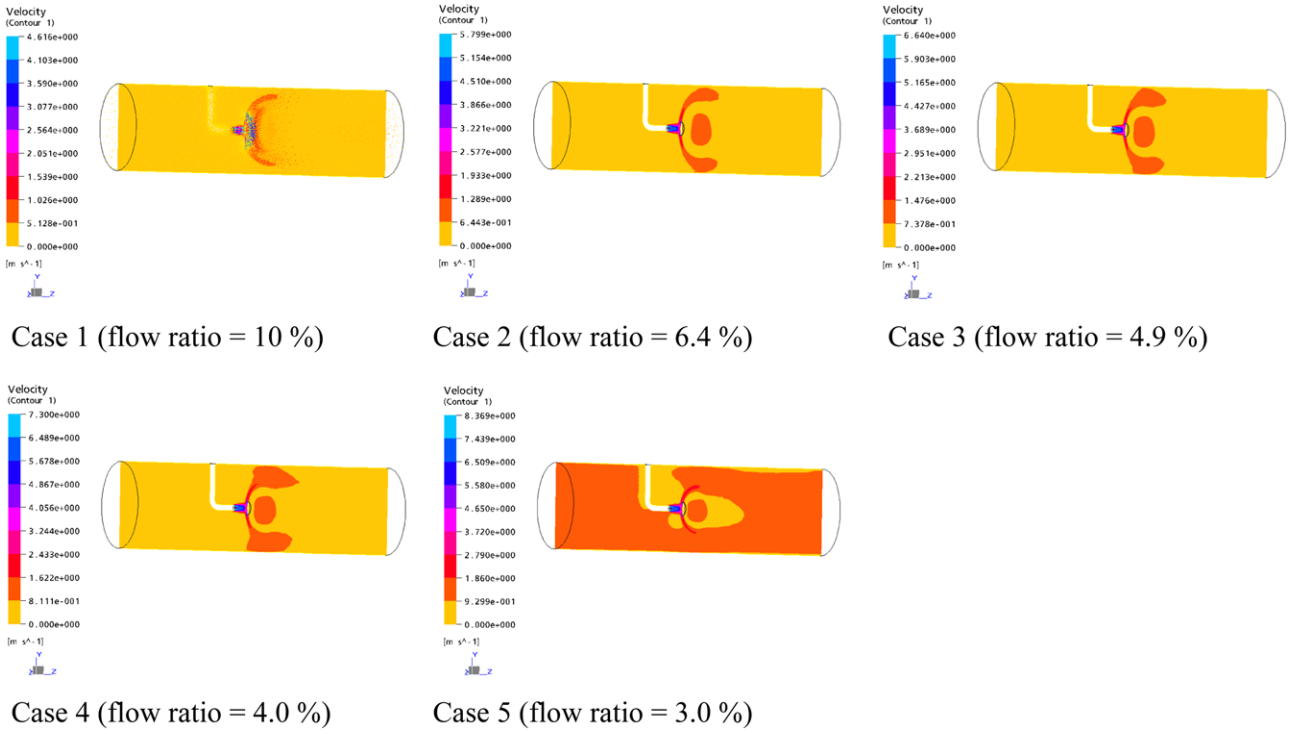

Fig. 6. The results of CFD simulation for case 1-5 (coagulant injection velocity=0.0001 m s^{-1}).

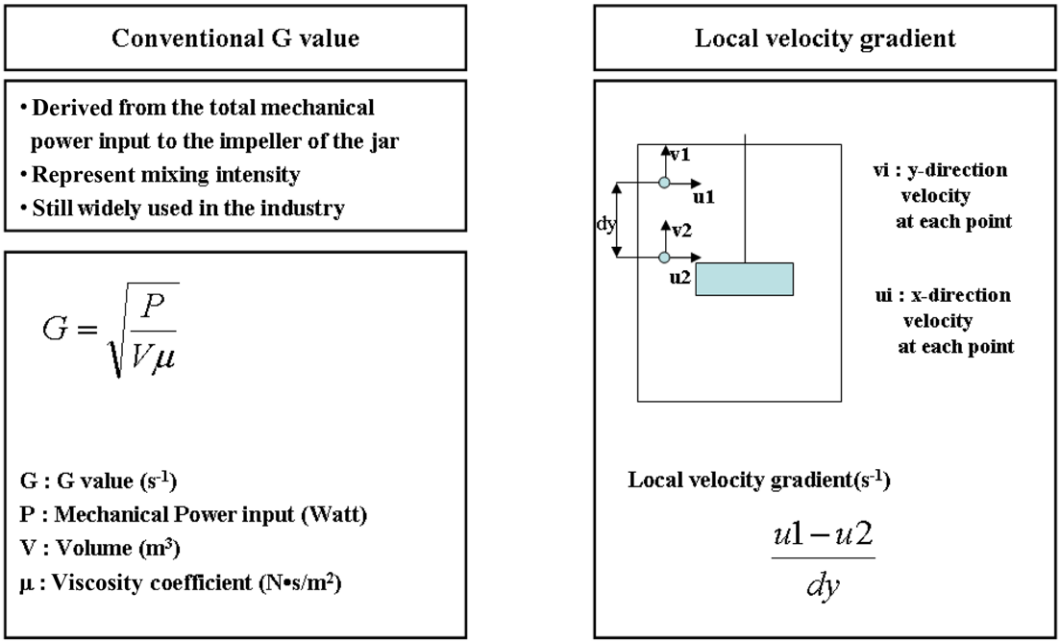

Fig. 7. The definitions of mean velocity gradient and local velocity gradient.

From the results of CFD simulation, it could be revealed that the higher the ratio of the pressurized flow to the constant water flow rate (Qi) becomes, the higher turbulent flow is observed in the rear region of the deflector. In the case of the flow ratio being the highest (12%) for each flow rate, the velocity difference between the main water and the pressurized water was largest. These results are similar with those from cases 1-5. Fig. 11 depicts the local velocity gradient just of cases 6 and 21 as the representatives for analyzing the results of CFD simulation quantitatively. Since a no-slip condition was assumed at the surface of the deflector, the local velocity gradient value was calculated to be zero on the y-axis (y-axis expresses the depth) of about −0.1-0.1 m.

As the results of calculation for velocity gradients, it could be concluded that the higher the flow ratio becomes, the larger the local velocity gradient is calculated on the data acquiring line. From the distribution of local velocity gradients in each case, Table 2 sum-

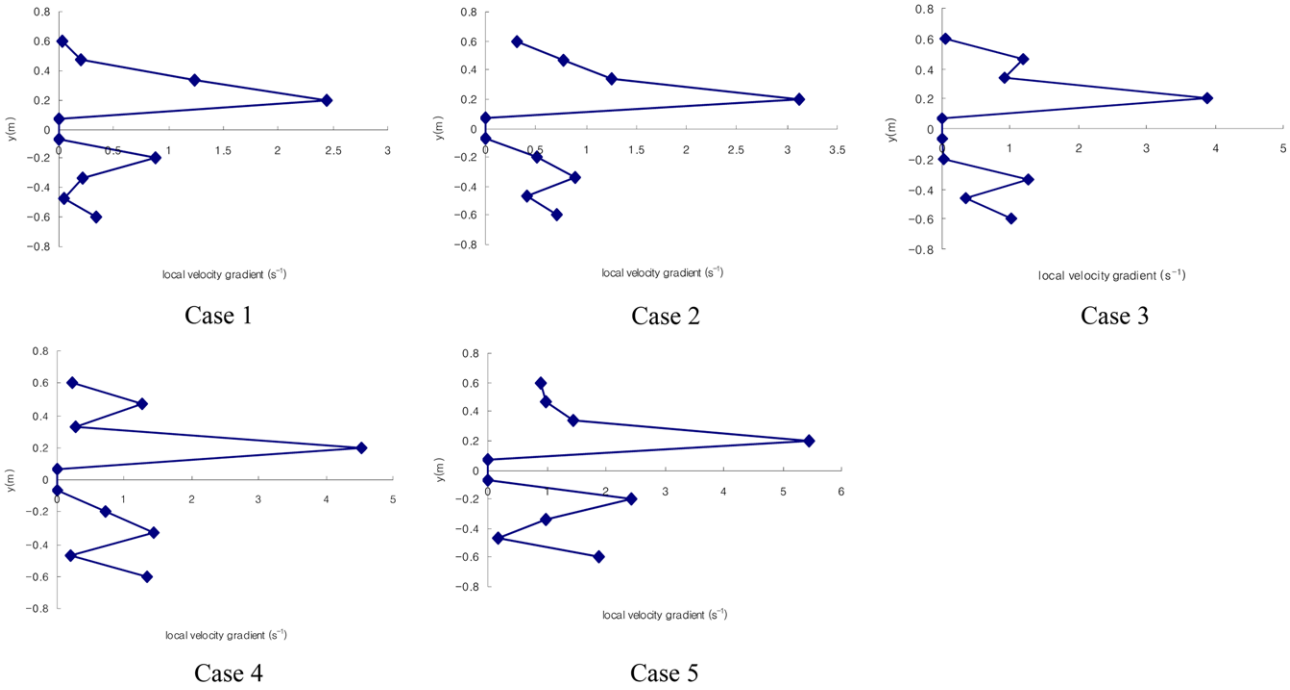

Fig. 8. The profiles of the calculated velocity gradients in cases 1-5.

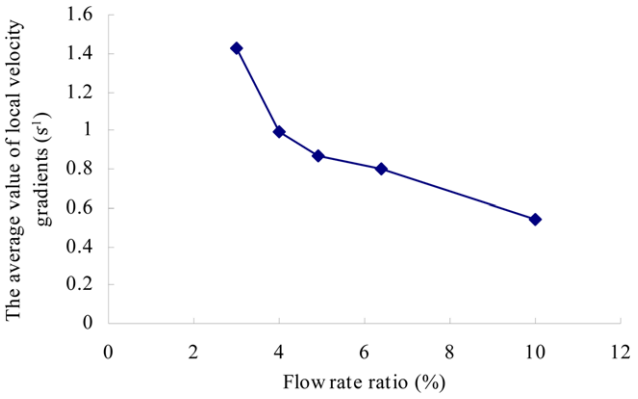

Fig. 9. The relationship between flow ratio and the average of local velocity gradients (cases 1-5).

marizes each condition and the average value of the distributed local velocity gradient.

Table 2 shows that the higher the flow ratio and the velocity ratio become for the constant flow rate (Qi), the higher the average value of local velocity gradient is calculated. From these results, it could be thought that the velocity ratio is adequate as the supplementary operating parameter to the flow ratio. It was observed that the average values of local velocity gradients have an apparent trend as velocity ratio changes as shown in Table 2, the fourth and last columns. As the velocity ratio increases for the constant main inlet flow, the average value of local velocity gradients might as well increase. For current operating conditions (cases 1-5) and virtual conditions (cases 6-21), the average value of local velocity gradient is dependent on the velocity ratio as well as the flow ratio. For example, Fig. 12 shows the relationship between the velocity ratio and the

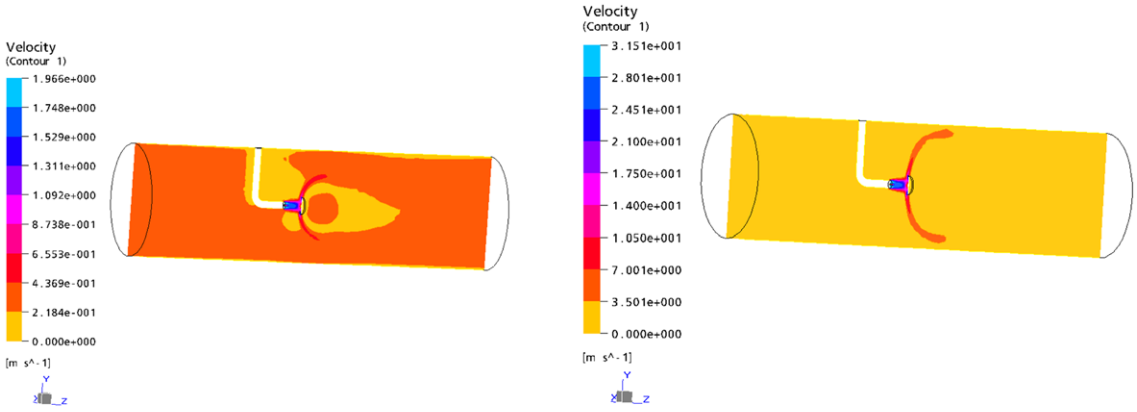

Fig. 10. The results of CFD simulation for case 6 and case 21.

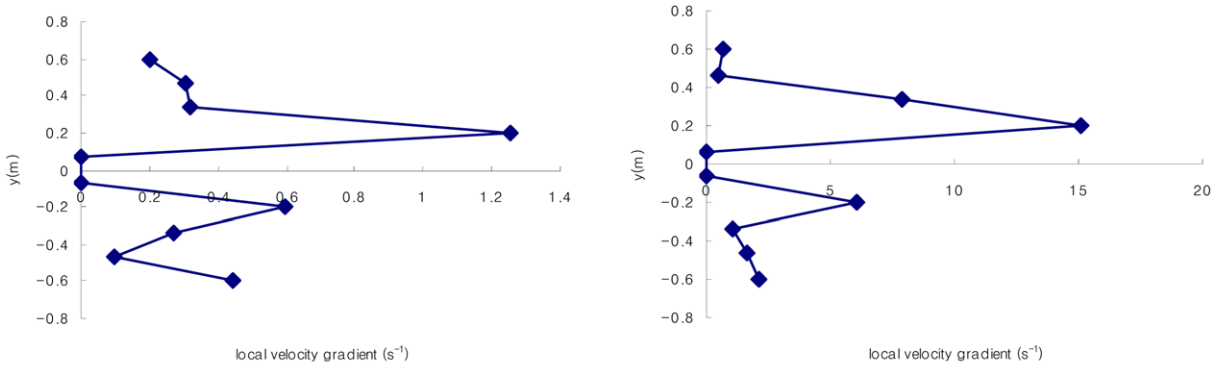

Fig. 11. The profiles of the calculated velocity gradients in case 6 and case 21.

Table 2. The relationship between operating conditions of PDM (case 6-21) and the average of local velocity gradients

Case	Main inlet water flow rate (Qi) ($m^3\ h^{-1}$)	Flow ratio (%)	Velocity ratio (dimensionless)	Average value of local velocity gradient (s^{-1})
Case 6	1,041	3.0	7.2	0.3484
Case 7	1,041	6.0	14.4	0.5475
Case 8	1,041	9.0	21.6	0.7557
Case 9	1,041	12.0	28.8	0.6300
Case 10	2,028	3.0	7.2	0.6747
Case 11	2,028	6.0	14.4	1.0702
Case 12	2,028	9.0	21.6	1.2461
Case 13	2,028	12.0	28.8	1.7501
Case 14	3,123	3.0	7.2	1.0296
Case 15	3,123	6.0	14.4	1.6404
Case 16	3,123	9.0	21.6	1.8600
Case 17	3,123	12.0	28.8	3.1175
Case 18	4,164	3.0	7.2	1.3502
Case 19	4,164	6.0	14.4	2.1915
Case 20	4,164	9.0	21.6	2.5906
Case 21	4,164	12.0	28.8	3.4957

average of local velocity gradients in cases 6, 7, 8, and 9 (the main inlet flow rate is 1,041 m^3/hr).

In the case that the main inlet flow rate is 1,041 m^3/hr, the peak velocity gradient was calculated at the velocity ratio of 21.6 (dimensionless). The velocity ratio, which shows the peak local velocity gradient, is a little bit different from other cases. In the other cases whose main inlet flow rates are 2,028 m^3/hr, 3,123 m^3/hr and 4,164 m^3/hr, the highest velocity gradients show up at a velocity ratio of 28.8 (dimensionless). The average value of the local velocity gradient increases steeply on the condition that the velocity ratios are in the rage of about 20-28 (dimensionless). From these results, it can be concluded that the velocity ratio (dimensionless) of the pressurized flow to the main inlet flow was as useful as the flow ratio in predicting the performance of PDM. In addition, the injected coagulant can be expected to disperse uniformly in the rare of deflector on the condition that the velocity ratio is over at least 20.

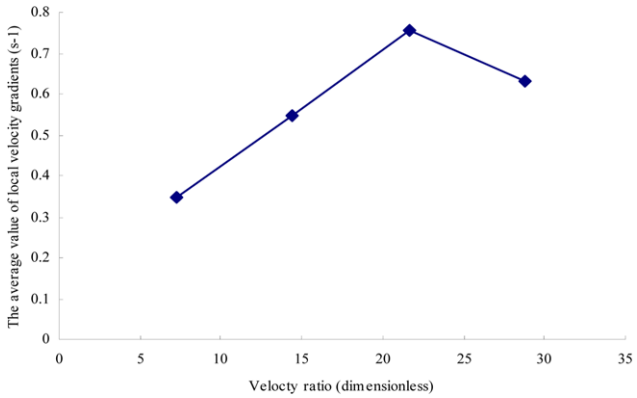

Fig. 12. The relationship between the velocity ratio and the average of local velocity gradients in cases 6, 7, 8 and 9.

SUMMARY

In this study, the authors evaluated the use of the ratio of the pressurized flow to the main inlet flow, which have been used as the important parameter for operating the pump diffusion mixer until now, using CFD simulation technique. Also, the authors suggested the velocity ratio (dimensionless) of the pressurized water to the main inlet water as a supplementary operating parameter and criterion (the velocity ratio of the pressurized flow to the main inlet flow should be greater than at least 20).

From the results of the wet test, the distribution of zeta potential in the case of velocity ratio about 22.2 was more uniform than any other case. This wet test could verify the results of CFD simulation.

From the simulation results of the case that the velocity ratio is about 21 (dimensionless), the average value of local velocity gradient is the highest. Also, the average value of local velocity gradient increases steeply on the condition that the velocity ratios are in the range of 20-28 (dimensionless). Consequently, if the velocity ratio is greater than at least 20, the performance of PDM, ultimately the uniform dispersion of coagulant, can be guaranteed.

REFERENCES

1. A. Amirtharajah and P. Mills, *J. AWWA*, **74**(5), 210 (1994).

2. H. E. Hudson and J. P. Wolfner, *J. AWWA*, **59**(10), 1257 (1967).
3. L. Vrale and R. M. Jorden, *J. AWWA*, **63**(1), 52 (1971).
4. S. Kawamura, *Integrated design of water treatment facilities*, John Wiley & Sons (1991).
5. H. Kim and S. Lee, *Sep. Purif. Technol.*, **52**, 117 (2006).
6. M. M. Clark, R. M. Srivastava, R. R. Lang, R. R. Trussell, L. J. McCollum, D. Bailey, J. D. Christie and G. Stolarik, *Selection and design of mixing processes for coagulation*, AWWA Research Foundation, Denver, USA (1994).
7. ANSYS, *CFX 10.0 Application manual*, Oxfordshire, United Kingdom (2006).
8. N. S. Park, H. Park and J. S. Kim, *J. Water Supply: Research & Technology -AQUA-*, **52**(2), 95 (2003).
9. H. K. Versteeg and W. Malalasekera, *An introduction to computational fluid dynamics*, Prentice-Hall, New Jersey (1995).
10. N. S. Park and H. Park, *Water Sci.Technol.: Water Supply*, **2**(5-6), 47 (2002).